Acta Cryst. (1954). 7, 153

The Interpretation of Diffuse X-ray Scattering from Powder Patterns of Solid Solutions*

BY P. A. FLINN,† B. L. AVERBACH AND P. S. RUDMAN

Department of Metallurgy, Massachusetts Institute of Technology, Cambridge, Massachusetts, U.S.A.

(*Received* 19 *January* 1953 *and in revised form* 18 *February* 1953)

Methods are developed for the evaluation of the Fourier coefficients which measure the local order and the sizes of atoms in solid solution. A transform of the diffuse scattering from polycrystalline samples modified by an exponential weighting function is used to obtain these coefficients with a minimum of false detail. Two experimental examples are given. Measurements of the diffuse intensity in electron units from an aluminum–zinc alloy at 400° C. show that zinc-rich clusters exist in the equilibrium solid solution above the solubility temperature. Similar measurements for a nickel–gold solid solution indicate a preference for unlike neighbors above the solubility gap. In the latter system the diffuse intensity produced by the difference in atomic radii is also observed.

Introduction

The diffuse X-ray scattering from solid solutions is affected by local atomic configurations and by differences in the atomic sizes. For a binary solution the diffuse intensity observed in a powder pattern as a result of these effects is given in electron units by

$$K(S) = \frac{I(S)}{Nm_A m_B (f_B - f_A)^2} - 1 = \sum_{i=1}^{\infty}{}' \left[C_i \alpha_i \frac{\sin Sr_i}{Sr_i} - C_i \beta_i \left(\frac{\sin Sr_i}{Sr_i} - \cos Sr_i \right) \right] \quad (1)$$

(Warren, Averbach & Roberts, 1951), where the prime on the summation indicates that the term for $i = 0$ is excluded and

S = $4\pi \sin\theta/\lambda$,
α_i ≡ $1 - p_i/m_A$ = short range order coefficients,
β_i ≡ $\left(\frac{1}{\eta - 1}\right)\left[-\left(\frac{m_A}{m_B} + \alpha_i\right)\varepsilon^i_{AA} + \left(\frac{m_B}{m_A} + \alpha_i\right)\eta\varepsilon^i_{BB} \right]$ = size effect coefficients,
ε^i_{AA} = $(r^i_{AA} - r_i)/r_i$, $\varepsilon^i_{BB} = (r^i_{BB} - r_i)/r_i$,
η = f_B/f_A,
θ = Bragg angle,
λ = irradiating wavelength,
r_i = average distance from a given atom to the ith shell of neighbors, determined from the lattice parameter and the crystal structure,
r^i_{AA} = distance from an A atom at the origin to another A atom in the ith shell,
r^i_{BB} = distance from a B atom at the origin to another B atom in the ith shell,
m_A = atom fraction of A atoms,
f_A = atomic scattering factor for an A atom,
C_i = number of atoms in the ith shell,
p_i = probability of finding an A atom in the ith shell about a B atom,
$I(S)$ = diffuse intensity in electron units.

The coefficients α_i describe the probability of finding an unlike neighbor in the ith shell about a given atom, and the coefficients β_i take into account the variations in the atomic sizes (Warren, Averbach & Roberts, 1951).

It has been the practice to evaluate these coefficients by a direct Fourier transformation of equation (1). Such a procedure is useful only when $\beta = 0$ (i.e. when the atoms have the same size) since in other cases the direct transform is difficult to interpret. An additional difficulty arises from the abrupt termination of the data at $S = S_0 \leqslant 4\pi/\lambda$. In practice the series may be terminated well before the function becomes negligible and this introduces false detail in the transform (Bragg & West, 1930; James, 1948*a*, *b*; van Reijen, 1951; Bertaut, 1952). It is shown in this paper that the secondary peaks of the false detail may contribute significantly to the apparent values of the higher coefficients. The transform is modified by an artificial temperature factor to minimize the false detail and to make possible the evaluation of both the α_i and the β_i coefficients. This method is applied to diffuse scattering measurements from aluminum–zinc and nickel–gold solid solutions.

False detail in the direct transform

For the case $\beta_i = 0$, a formal sine Fourier transform has been used to evaluate the coefficients α_i. Wilchinsky (1944) defines a function $U(r)$ such that

* This work was performed under the sponsorship of the U.S. Atomic Energy Commission under Contract AT(30-1)-1002 and represents a portion of the dissertation presented by P. A. Flinn for the degree of Sc.D. at the Massachusetts Institute of Technology.

† Present address: Department of Physics, Wayne University, Detroit, Michigan, U.S.A.

$$\int_{r_i-\delta}^{r_i+\delta} U(r)dr = C_i\alpha_i \,. \qquad (2a)$$

Replacing the summation in equation (1) by an integral, we obtain

$$K(S) = \int_0^\infty U(r)\frac{\sin Sr}{Sr}dr \,. \qquad (2b)$$

Performing a Fourier transformation,

$$\frac{U(r)}{r} = \frac{2}{\pi}\int_0^\infty SK(S)\sin Sr\,dS = (2/\pi)f(r) \qquad (3)$$

and

$$C_i\alpha_i = \frac{2}{\pi}\int_{r_i-\delta}^{r_i+\delta} rf(r)dr \,. \qquad (4)$$

In practice, the evaluation of $C_i\alpha_i$ cannot be carried out rigorously by an application of equation (4) since the function $K(S)$ can be obtained experimentally only for values of S up to a limiting value S_0, where $S_0 < 4\pi/\lambda$. The effects of this restriction may be seen by integrating the function $f(r)$ directly between finite limits. The integral in equation (3) becomes

$$\int_0^{S_0} SK(S)\sin Sr\,dS = f_0(r) = \sum_{i=1}^{\infty}{}' \frac{(C_i\alpha_i)_0}{r_i}\int_0^{S_0}\sin Sr_i \sin Sr\,dS \,, \qquad (5)$$

where $(C_i\alpha_i)_0$ refers to the experimental values obtained when only data to S_0 are included.

The integration is given by

$$\int_0^{S_0}\sin Sr_i\sin Sr\,dS = \frac{\sin S_0v_i}{2v_i} - \frac{\sin S_0w_i}{2w_i} \,, \qquad (6)$$

$$v_i = r-r_i \quad \text{and} \quad w_i = r+r_i \,.$$

The term containing v_i has a sharp peak at $r = r_i$ with a series of secondary peaks on either side, and this function is shown in Fig. 1. The term containing w_i has similar peaks at $r = -r_i$ and these may be disregarded except as the source of minor fluctuations near the origin. Equation (5) thus becomes

$$f_0(r) = \sum_{i=1}^{\infty}{}' \frac{(C_i\alpha_i)_0}{r_i}\left[\frac{\sin S_0v_i}{2v}\right] \,. \qquad (7a)$$

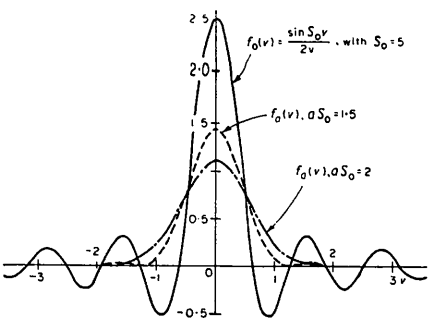

Fig. 1. Effect of artificial temperature factor on short-range order peak.

For a given value of i we may take the area under the function $f_0(r)$ in the interval $(r_i-\delta)$ to $(r_i+\delta)$, and we obtain

$$(C_i\alpha_i)_0 = \frac{r_i\int_{r_i-\delta}^{r_i+\delta} f_0(r)\,dr}{\int_{-\delta}^{\delta}(\sin S_0v_i)/2v_i dv_i} \,. \qquad (7b)$$

If the interval δ extends far enough to include the entire function, the area $\int_{-\infty}^{\infty}(\sin S_0v_i)/2v_i dv_i$ equals $\pi/2$, equation (7b) becomes comparable with the formal Fourier transform of equation (4) and $C_i\alpha_i = (C_i\alpha_i)_0$. In practice, however, the value of δ is taken to include only the area under the principal peak. The denominator in equation (7b) then becomes 1·85 (Jahnke & Emde, 1945, Table 1), independent of S_0, and

$$(C_i\alpha_i)_{0,p} = \frac{r_i}{1{\cdot}85}\left[\int_{r_i-\delta}^{r_i+\delta} f_0(r)dr\right]_{\text{principal peak}} \,. \qquad (7c)$$

Thus, if the values of α_i are obtained from the principal peak using data to S_0, but equation (4) is used, the values of $C_i\alpha_i$ will then be in error by about 18%.

It is unnecessary to include the entire peak in order to evaluate α_i; the value of δ may be chosen large enough to describe the central portion but small enough to avoid interference effects near the ends of the transform peak and equation (7b) may be evaluated directly. In the application of equation (4) the area $\int rf(r)dr$ is used rather than the area $r_i\int f_0(r)dr$ in accordance with equation (7). Since $f_0(r)$ is symmetrical about r_i the result is the same by either procedure.

This method is satisfactory only if the secondary maxima associated with adjacent peaks do not interfere. Unfortunately such interference is usually present and the secondary peak associated with α_1 comes at the same place as the short range order peak associated with α_2. This may be shown as follows. The first negative peak of the function $(\sin S_0v_i)/v_i$ occurs when the argument is about 4·5. The largest value of S_0 attainable experimentally is about 5. The first peak in the false detail thus comes at $r-r_i = 0{\cdot}9$ Å, and in many of the common metals this distance is approximately equal to the difference between the radii of the first and second shells of atoms. The first spurious peak thus appears in about the same place as the peak associated with α_2, which describes the short-range order of second neighbors.

The area of the first negative peak of $(\sin S_0v_i)/v_i$ is about 8% of the principal peak. If this spurious peak is misinterpreted as arising from a second neighbor order term, $C_2\alpha_2$,

$$C_2\alpha_2/r_2 = -(0{\cdot}08)C_1\alpha_1/r_1 \,.$$

If we take $r_2/r_1 = 1{\cdot}5$, then $C_2\alpha_2 = C_1\alpha_1/8$. Taking $C_1 = 12$ and $C_2 = 6$ as in the face-centered cubic

structure $\alpha_2 = -\alpha_1/4$. This is of the same order as the values usually reported for α_2 and this fact should be considered in interpreting powder data. It should be noted that this effect does not arise from errors in measurement but simply from the abrupt termination of the transform.

The modified transform

If the atoms differ in size it is also necessary to evaluate the β_i coefficients. We let $\gamma_i = \alpha_i - \beta_i$ and equation (1) becomes

$$\int_0^{S_0} SK(S)\sin SrdS = f_0(r) = \sum_{i=1}^{\infty}{}' \frac{C_i\gamma_i}{r_i}\int_0^{S_0}\sin Sr_i \sin SrdS + \sum_{i=1}^{\infty}{}' C_i\beta_i\int_0^{S_0} S\cos Sr_i \sin SrdS . \quad (8)$$

The last integral becomes

$$\int_0^{S_0} S\cos Sr_i\sin SrdS = \frac{S_0}{2v_i}\left(\frac{\sin S_0v_i}{S_0v_i} - \cos S_0v_i\right) + \frac{S_0}{2w_i}\left(\frac{\sin S_0w_i}{S_0w_i} - \cos S_0w_i\right), \quad (9)$$

and, as before, we may neglect the terms in w_i. The behavior of the term containing v_i in equation (9) is shown in Fig. 2. The invariant of this function might

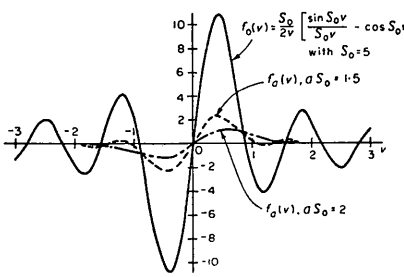

Fig. 2. Effect of artificial temperature factor on size-effect peaks.

be expected to be the first moment, just as the invariant for the function in equation (6) is the area. The moment fails to converge, however, and β_i cannot be conveniently evaluated from this transform. The secondary peaks are also quite prominent for this type of function.

The difficulties arising from false detail and the presence of β_i coefficients may be overcome by the introduction of an artificial temperature factor of the form $\exp(-a^2S^2)$. Equation (8) becomes

$$\int_0^{S_0} SK(S)\exp(-a^2S^2)\sin SrdS = f_a(r) = \sum_{i=1}^{M}{}' \frac{C_i\gamma_i}{r}\int_0^{S_0}\exp(-a^2S^2)\sin Sr_i\sin SrdS + \sum_{i=1}^{M}{}' C_i\beta_i\int_0^{S_0}\exp(-a^2S^2)S\cos Sr_i\sin SrdS . \quad (10)$$

Each of the integrals in equation (10) may be evaluated by means of contour integration in the complex plane. For the first integral we obtain

$$\int_0^{S_0}\exp(-a^2S^2)\sin Sr_i\sin SrdS = \frac{\sqrt{\pi}}{4a}\exp(-v_i^2/4a^2) + P_1(v_i/2a, aS_0)\sin S_0v_i + P_2(v_i/2a, aS_0)\cos S_0v_i , \quad (11)$$

where the functions P_1 and P_2 are evaluated in Appendix A. Terms in w_i are neglected as before. The right-hand portion of equation (11) is shown in Fig. 1 for two values of a. The exponential term gives rise to a Gaussian peak about $r = r_i$ in place of the $(\sin S_0v)/v$ curve. The secondary peaks come from the functions P_1 and P_2, and these may be made arbitrarily small by choosing a sufficiently large value for aS_0. Since the value of S_0 is fixed by the experiment, only a may be increased. However, increasing the value of a broadens the transform and reduces the resolution. Fig. 1 shows that a choice of $(aS_0) = 2$ suppresses the secondary peaks quite well; a value of $(aS_0) = 1{\cdot}5$ gives almost as good resolution as the unmodified transform with only small secondary fluctuations.

The second integral becomes

$$\int_0^{S_0}\exp(-a^2S^2)S\cos Sr_i\sin SrdS = \frac{\sqrt{\pi}}{8a^3}v_i\{\exp(-v_i^2/4a^2) + [P_1 + (2a/v_i\sqrt{\pi})\exp(-a^2S_0^2)]\sin S_0v_i + P_2\cos S_0v_i\}. \quad (12)$$

Terms in w_i are also neglected here. This function is also shown in Fig. 2 for $(aS_0) = 1{\cdot}5$ and $(aS_0) = 2$. The dominant term has the shape of the derivative of the error function and the secondary peaks are similar to those considered previously.

If we choose a value of $(aS_0) = 1{\cdot}5$ or larger, the contributions of the functions P_1 and P_2 may be neglected. Equation (10) becomes

$$\int_0^{S_0} SK(S)\exp(-a^2S^2)\sin SrdS = f_a(r) = \sum_{i=1}^{M}{}' \frac{C_i\gamma_i}{r_i}\left\{\frac{\sqrt{\pi}}{4a}\exp(-v_i^2/4a^2)\right\} + \sum_{i=1}^{M}{}' C_i\beta_i\left\{\frac{\sqrt{\pi}\,.\,v_i}{8a^3}\exp(-v_i^2/4a^2)\right\} . \quad (13)$$

The function $f_a(r)$ is evaluated from the experimental data. Taking the area under the function in the interval $r_i - \delta$ to $r_i + \delta$, we obtain

$$\int_{r_i-\delta}^{r_i+\delta} f_a(r)dr = \frac{C_i\gamma_i}{r_i}\int_{-\delta}^{\delta}\frac{\sqrt{\pi}}{4a}\exp(-v_i^2/4a^2)dv = \frac{C_i\gamma_i}{r_i}\left\{\frac{\pi}{2}\varphi(\delta/2a)\right\} , \quad (14)$$

where $\varphi(\delta/2a)$ is the error integral, and thus

$$C_i\gamma_i = \frac{2r_i}{\pi\varphi(\delta/2a)}\int_{r_i-\delta}^{r_i+\delta} f_a(r)dr . \quad (14a)$$

It should be noted that the function containing β_i explicitly does not contribute to the area.

If δ is chosen large enough to include the entire area under the peak, $\varphi(\delta/2a)$ may be taken as unity. If there is too much interference near the tails of the peak arising from the adjacent peaks, the interval δ may be chosen large enough to describe adequately the central portion of the peak, but not large enough to be affected by the interference. The area from $r_i-\delta$ to $r_i+\delta$ is measured, the function $\varphi(\delta/2a)$ is evaluated from existing tables and the values of γ_i are calculated from equation (14a).

If we form the first moment of $f_a(r)$ about r_i we obtain

$$\int_{r_i-\delta}^{r_i+\delta} f_a(r)(r-r_i)dr = \int_{-\delta}^{\delta} C_i\beta_i(\sqrt{\pi}/8a^3)v_i^2 \exp(-v_i^2/4a^2) . \tag{15}$$

On integration by parts,

$$\frac{\sqrt{\pi}}{8a^3}\int_{-\delta}^{\delta} v_i^2 \exp(-v_i^2/4a^2) = (\pi/2)\varphi(\delta/2a)-(\sqrt{\pi}/2)[(\delta/a)\exp(-\delta^2/4a^2)] . \tag{16}$$

Thus

$$C_i\beta_i = \frac{2}{\pi\varphi(\delta/2a)-\sqrt{\pi}[(\delta/a)\exp(-\delta^2/4a^2)]} \times \int_{r_i-\delta}^{r_i+\delta} f_a(r)(r-r_i)dr . \tag{17}$$

It should be noted that the first moment of the terms containing the γ_i coefficients is zero and that the introduction of the exponential weighting factor has produced a convergent first moment for the twin peaks associated with the size effect. If the resolution is adequate ($\delta/2a$) may be taken large enough so that $\varphi(\delta/2a)$ approaches unity and the second term in the denominator is negligible. The moment of the entire peak may then be taken about r_i. The resolution is seldom this good and to avoid interference the interval δ may be taken only to include the central portion of the twin peaks and equation (17) evaluated for the chosen values of δ and a.

The coefficients β_i and γ_i may thus be determined from the first moment and the area, respectively, of the function $f_a(r)$. If β_i is small compared with α_i, the characteristic double peak of the size-effect transform may be obscured and the resultant peak will merely seem unsymmetric about r_i. If the presence of the size effect is ignored an erroneous value of α_i may be obtained since the area under the peak is proportional to $\gamma_i = \alpha_i-\beta_i$.

Effects of errors in the data

One of the principal advantages of the Fourier transformation in the interpretation of diffuse X-ray scattering phenomena is the separation of certain disturbances in the original data to regions in the transform where they do not seriously affect the final results. This may be shown by considering the effect of any general error which might be present in addition to the true diffuse scattering. Such an error may be approximated in the mean arbitrarily well by using a sufficient number of terms in the expression

$$E(S) = \sum_{n=1}^{N}(A_n \sin Sr_n + B_n \cos Sr_n) , \tag{18}$$

where (r_n) may have any values. (This is not a Fourier series.) If such an error is added to the diffuse intensity, the modified transform of the error will be added to the true transform. For the error transform,

$$\int_0^{S_0} S\exp(-a^2S^2)E(S)\sin SrdS = g(r) = \sum_1^N A_n\int_0^{S_0} S\exp(-a^2S^2)\sin Sr\sin Sr_n dS + \sum_1^N B_n\int_0^{S_0} S\exp(-a^2S^2)\sin Sr\cos Sr_n dS . \tag{19}$$

The second of these integrals has already been evaluated; it is essentially the same as equation (12). The first integral is evaluated by similar methods. We thus have

$$g(r) = \sum_1^{N}{}' A_n(\sqrt{\pi}/8a^3)\{v_nG(v_n/2a)-w_nG(w_n/2a)\} + \text{small terms in } P_1 \text{ and } P_2 + \sum_1^{N}{}' B_n(\sqrt{\pi}/8a^3)\{v_n\exp(-v_n/4a^2)+w_n\exp(-w_n/4a^2)\} + \text{small terms in } P_1 \text{ and } P_2 , \tag{20}$$

where

$$G(t) = (2/\sqrt{\pi})\exp(-t^2)\int_0^t \exp(y^2)dy;$$

$$v_n = r-R_n,\ w_n = r+R_n .$$

These functions have appreciable values only for small values of v_n; that is for values of r close to R_n. Consequently, errors which are slowly varying functions of S, which have correspondingly small values of r_n, give rise to disturbances in the transform which are confined to the neighborhood of the origin. Very rapidly varying errors, with high values of r_n, will

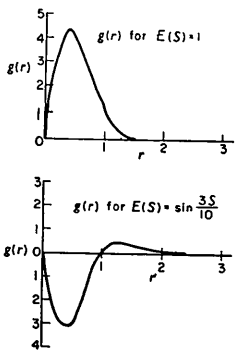

Fig. 3. Error transforms. Upper: for constant error; lower: for sinusoidal error added to the diffuse intensity.

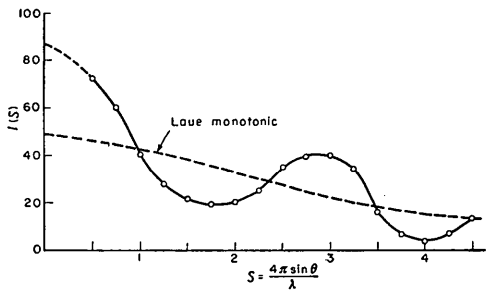

Fig. 4.

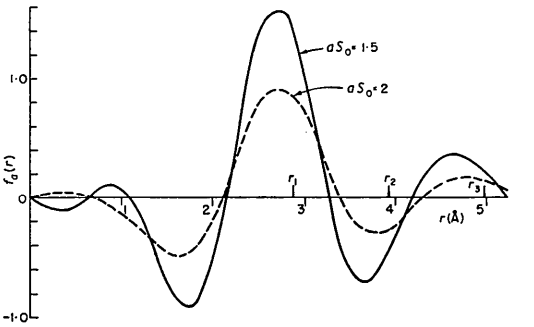

Fig. 5.

Fig. 4. Diffuse scattering in electron units for aluminum–30 atomic % zinc alloy at 400° C. Temperature-diffuse and Compton modified scattering subtracted. Co $K\alpha$ radiation at 22 kV. monochromated with bent fluorite crystal.

Fig. 5. Modified Fourier transform of diffuse intensity from aluminum–30 atomic % zinc alloy at 400° C., showing effect of weighting function. $\alpha_1 = 0{\cdot}20$ and $\beta_1 = -0{\cdot}005$.

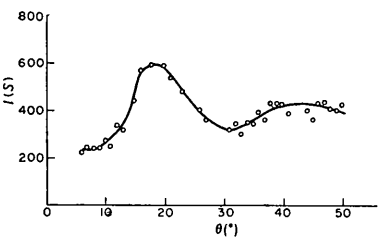

Fig. 6.

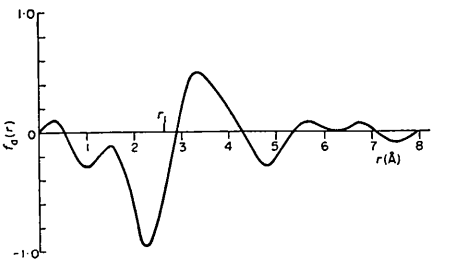

Fig. 7.

Fig. 6. Diffuse intensity in electron units from 0·7 nickel–0·3 gold alloy (atomic fractions). Quenched from 900° C. and measured at −190° C. Temperature-diffuse and Compton modified scattering subtracted. Co $K\alpha$ radiation at 22 kV. monochromated with bent fluorite crystal.

Fig. 7. Modified Fourier transform of diffuse intensity from 0·7 nickel–0·3 gold alloy quenched from 900° C. with $aS_0 = 1{\cdot}5$, $\alpha_1 = -0{\cdot}03$ and $\beta_1 = 0{\cdot}03$.

produce disturbances far out in the transform. Only those components of the error which vary with a periodicity close to that of the effect being studied will cause serious interference with the peak. The appearance of the error transforms for constant error and for error increasing monotonically with (S) are shown in Fig. 3. It may be seen that these correspond closely with the disturbances near the origin observed for the transforms of the experimental data.

Examples of short-range order and size effect

The application of the modified transform to a case where the size effect is virtually absent may be illustrated by treating the data from aluminum–zinc solid solutions. Typical diffuse-scattering data from an alloy containing 30 atomic % zinc taken at 400° C. with monochromatic Co $K\alpha$ radiation by a combination of photographic and Geiger-counter spectrometer techniques are shown in Fig. 4. At this temperature the alloy is single phase and face-centered cubic. The intensity is given in electron units (intensity was calibrated by measuring the scattering from lucite) and temperature-diffuse as well as Compton modified scattering have been subtracted.

Modified transforms of the data in Fig. 4 are shown in Fig. 5. Two different damping constants have been used, and the reduction in the spurious peaks as a is increased is apparent. The minor fluctuations which appear in the modified transform came from errors in the data, particularly from the imperfect correction for the temperature-diffuse scattering. Since these minor fluctuations do not correspond to distances of the order of r_i, they cannot be attributed to order. In the evaluation of α_1, δ was taken as 0·5 Å, the area under each curve was measured for the interval $r_1-\delta$ to $r_1+\delta$, the function $\varphi(\delta/2a)$ was evaluated, and the values of α_1 and β_1 were obtained from equations (14) and (17). Values of $\alpha_1 = 0{\cdot}2$ and $\beta_1 = -0{\cdot}005$ were obtained. Since the value of β_1 is within the experimental error it was neglected, and the aluminum and zinc atoms are considered to have the same size in solid solution. The same value for α_1 was obtained from each of the damped curves in Fig. 5.

The measured value of α_1 indicates that, in this solution on the average, each zinc atom has 5·3 zinc nearest neighbors instead of the 3·6 like neighbors which would be found in a random solution. This may be interpreted as evidence for the existence of zinc-rich regions in the crystal, and represents the opposite of the type of short-range order found in copper–gold alloys above the critical temperature. In the latter

case there is a preference for unlike nearest neighbors and α_1 is negative. Small-angle scattering similar to that shown in Fig. 4 was observed for aluminum alloys containing 5–50 atomic % zinc in measurements at 400° C. It thus appears that these single-phase solutions contain zinc-rich clusters in equilibrium above the solubility temperature.

The scattering from nickel–gold solid solutions provides an excellent illustration of the case in which size effect is large. Fig. 6 shows the diffuse scattering from a 0·7 nickel–0·3 gold (atomic %) solid solution, and Fig. 7 shows the corresponding transform. The nonsymmetric twin peak in the neighborhood of r_1 arises from the combination of a symmetric twin peak corresponding to a positive β_1, and a Gaussian negative peak corresponding to a negative γ_1. Using the methods described above, β_1 is found to be +0·03, and $\alpha_1 = -0{\cdot}03$. The other peaks in the transform are not associated with interatomic spacings in the alloy, and must be attributed to errors in the data.

The coefficients α_1 and β_1 have been studied as a function of composition for the gold–nickel system at temperatures above the solubility gap. The sign of α_1 was always negative, indicating a preference for unlike neighbors, despite the fact that these solutions precipitate solutions rich in nickel and solutions rich in gold on cooling. From the values of β_1 as a function of composition it was possible to find the sizes of the nickel and gold atoms in solution, and these results are reported elsewhere. The negative values of α_1 in nickel–gold solutions indicate that these alloys might undergo an order–disorder transformation similar to that in copper–gold if the atom sizes were not so dissimilar. It is surmised that the decomposition into nickel-rich and gold-rich solutions on cooling occurs in order to minimize the lattice strain energy arising from the difference in atomic sizes.

The authors are grateful to the U.S. Atomic Energy Commission for their support of this program and to Mr Mathias Comerford for his assistance with the experimental determinations.

APPENDIX A

The functions P_1 and P_2 are given by

$$P_1(t, aS_0) = \frac{2}{\sqrt{\pi}}\int_0^t \exp(-t^2)\exp\left(y^2 - \frac{a^2S_0^2t^2}{y^2}\right)dy \quad (A\text{-}1)$$

and

$$P_2(t, aS_0) = \frac{-2aS_0t}{\sqrt{\pi}}\int_0^t \exp(-t^2)\exp\left(y^2 - \frac{a^2S_0^2t^2}{y^2}\right)\frac{dy}{y^2}, \quad (A\text{-}2)$$

where $t = v/2a$.

P_1 and P_2 may be evaluated by making use of an approximate series given by Miller & Gordon (1931):

$$P_1(t, aS_0) = F(t)/\pi - \tfrac{1}{2}\exp(-t^2)\tan aS_0t + \frac{1}{aS_0t}\sum_{\substack{m=1\\ \text{odd}}}^{\infty}[\exp(-m^2\pi^2/4a^2S_0^2)]/[m^2\pi^2/(2aS_0t)^2 - 1], \quad (A\text{-}3)$$

where $F(t)$ is a function tabulated in the reference cited. We obtain a series for P_2 by partially differentiating (A-3) with respect to (aS_0t), giving

$$P_2(t, aS_0) = (\sqrt{\pi}/4)\left[-\tfrac{1}{2}\exp(-t^2) - \tfrac{1}{2}\exp(-t^2)\tan^2 aS_0t + \frac{1}{(aS_0t)^2}\sum_{\substack{m=1\\ \text{odd}}}^{\infty}\left\{2\left(\frac{m}{2aS_0}\right)^2 + \frac{(m\pi/2aS_0t)^2+1}{(m\pi/2aS_0t)^2-1}\left/\frac{\exp(-m^2\pi^2/4a^2S_0^2t^2)}{(m\pi/2aS_0t)^2-1}\right.\right\}\right]. \quad (A\text{-}4)$$

Some values of P_1 and P_2 are tabulated in Table 1. To guard against gross errors, some points were checked by direct numerical integration of (A-1) and (A-2).

Table 1(a). *Values of* $P_1(v/2a, aS_0)$

$v/2a$	$aS_0 = 1{\cdot}5$	$aS_0 = 2{\cdot}0$	$aS_0 = 2{\cdot}5$
0·5	$8{\cdot}5\times10^{-3}$	$9{\cdot}5\times10^{-4}$	$7{\cdot}2\times10^{-5}$
1·0	$1{\cdot}4\times10^{-2}$	$1{\cdot}7\times10^{-3}$	$1{\cdot}3\times10^{-4}$
1·5	$1{\cdot}7\times10^{-2}$	$2{\cdot}2\times10^{-3}$	$1{\cdot}7\times10^{-4}$
2·0	$1{\cdot}8\times10^{-2}$	$2{\cdot}4\times10^{-3}$	$1{\cdot}9\times10^{-4}$
2·5	$1{\cdot}7\times10^{-2}$	$2{\cdot}5\times10^{-3}$	$2{\cdot}1\times10^{-4}$
3·0	$1{\cdot}6\times10^{-2}$	$2{\cdot}4\times10^{-3}$	$2{\cdot}1\times10^{-4}$

Table 1(b). *Values of* $P_2(v/2a, aS_0)$

$v/2a$	$aS_0 = 1{\cdot}5$	$aS_0 = 2{\cdot}0$
0	$3{\cdot}4\times10^{-2}$	$4{\cdot}8\times10^{-3}$
0·5	$3{\cdot}2\times10^{-2}$	$4{\cdot}5\times10^{-3}$
1·0	$2{\cdot}8\times10^{-2}$	$4{\cdot}0\times10^{-3}$
1·5	$2{\cdot}2\times10^{-2}$	$3{\cdot}4\times10^{-3}$
2·0	$1{\cdot}6\times10^{-2}$	$2{\cdot}7\times10^{-3}$
2·5	$1{\cdot}2\times10^{-2}$	$2{\cdot}1\times10^{-3}$
3·0	$1{\cdot}0\times10^{-2}$	$2{\cdot}0\times10^{-3}$

References

Bertaut, E. F. (1952). *Acta Cryst.* **5**, 387.

Bragg, W. L. & West, J. (1930). *Phil. Mag.* (7), **10**, 823.

Jahnke, E. & Emde, F. (1945). *Funktionentafeln*, 4th ed. New York: Dover Publications.

James, R. W. (1948*a*). *Acta Cryst.* **1**, 132.

James, R. W. (1948*b*). *The Optical Principles of the Diffraction of X-rays*, chap. 7. London: Bell.

Miller, W. L. & Gordon, A. R. (1931). *J. Phys. Chem.* **35**, 2785.

Reijen, L. L. van (1951). *Selected Topics in X-ray Crystallography*, chap. 3. Amsterdam: North Holland Publishing Co.

Warren, B. E., Averbach, B. L. & Roberts, B. W. (1951). *J. Appl. Phys.* **22**, 1493.

Wilchinsky, Z. (1944). *J. Appl. Phys.* **15**, 806.